TABLE III. $C(T)$ for copper (in units of 10^2 eV^{-1}).

T(°K)	Flinn *et al.* Experimental values θ_D	$C(T)$	C.F. model	Jacobsen	White	A-S	Debye model θ_D=335°K
4	320±10	0.544∓0.02	0.552	0.579	0.537	0.570	0.520
20	320±10	0.588∓0.02	0.566	0.593	0.548	0.582	0.532
80	320±10	0.755∓0.04	0.762	0.808	0.733	0.779	0.697
300	315±10	2.17 ∓0.14	2.10	2.29	2.03	2.18	1.93
400	300±10	3.14 ∓0.25	2.77	3.02	2.67	2.87	2.50

for aluminum determined by Walker from his experimental dispersion curves. The experimental and calculated temperature dependence of $C(T)$ for copper is given in Table III. For comparison we calculated $C(T)$ using a Debye model, the results of these calculations are also shown in this table.

From the results in Table III we conclude that the experimental determination of the Debye-Waller factor for pure host lattices of cubic symmetry is not sensitive enough to distinguish between the various models. Models inconsistent with experimental dispersion curves such as the C.F. model and White's full tensor model give essentially the same Debye-Waller factor.

The results of the calculations for aluminum using Walker's force constants are given in Table IV. Using the A-S force constants the values of $C(T)$ are higher than Walker's by 1% at 0°K and by 4% at 400°N. Only a small difference is expected since Walker's constants are essentially axially symmetric.

TABLE IV. $C(T)$ for aluminum (in units of 10^2 eV^{-1}).

T(°K)	Walker	Debye model (θ_D=382°K)
4	0.471	0.459
20	0.478	0.464
80	0.598	0.583
300	1.54	1.50
400	2.02	1.96

PHYSICAL REVIEW VOLUME 131, NUMBER 2 15 JULY 1963

Temperature Dependence and Anisotropy in the Debye-Waller Factor for White Tin

R. E. DEWAMES, T. WOLFRAM, AND G. W. LEHMAN
North American Aviation Science Center, Canoga Park, California
(Received 11 March 1963)

The Debye-Walker factor, e^{-2W}, for tin is calculated using the A-S (axially symmetric) lattice dynamics model described in an earlier paper. The Debye continuum approximation is found to be unsatisfactory because the optical modes contribute significantly even at low temperatures. Calculated and experimental values determined from Mössbauer measurements are in excellent agreement in the temperature range from 0 to 300°K. Discrepancies above 300°K are attributed to higher order corrections such as anharmonicities and diffusion effects. In tin, the Debye-Waller factor depends upon the direction of gamma ray emission with the ratio $2W_x/2W_z$ varying from 1.1 to 1.2 for T=0°K and T=300°K, respectively. The calculated anisotropy in $2W$ is compared with available experimental data. Dispersion curves and values of $2W$ calculated using Rayne and Chandrasekhar elastic data are compared with those calculated using Mason and Bömmel elastic data. The effect of the relative motion of the two sublattices on the elastic properties of tin is discussed and found to be important for the elastic constants of Rayne and Chandrasekhar.

I. INTRODUCTION

THE probability of a gamma-ray emission without energy transfer to or from the lattice[1,2] and the temperature dependence of the atomic structure factor in the reflection of x rays[3] is given by

$$f=e^{-2W} \tag{1}$$

where $2W$ is related to the mean square displacement of an atom along a definite direction.

Since the experimental determination of f for tin has only been investigated through a study of the temperature dependence of recoil-less γ emission the constant $2W$ is defined for this specific case. Hence,

$$2W=R\sum_q\sum_j[\mathbf{e}^\alpha\cdot\mathbf{e}^\alpha(q,j)]^2g[\omega(q,j)], \tag{2}$$

[1] R. L. Mössbauer, Z. Physik **151**, 124 (1958).
[2] W. E. Lamb, Jr., Phys. Rev. **55**, 190 (1939).
[3] R. W. James, *The Optical Principles of the Diffraction of X-Rays* (G. Bell and Sons, London, 1953).

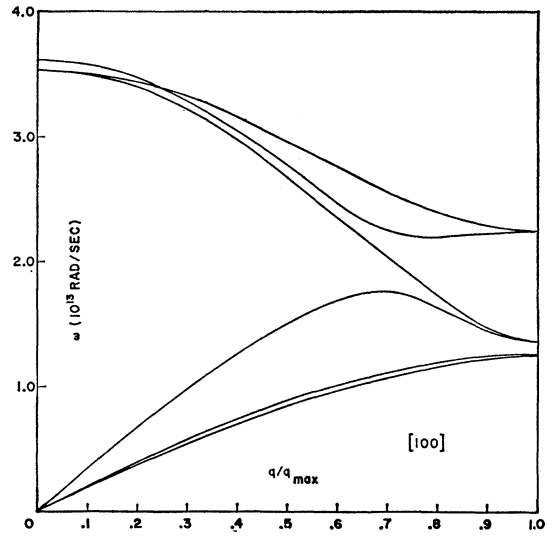

FIG. 1. Dispersion curves for white tin along [100] direction in the Brillouin zone using Rayne and Chandrasekhar elastic data.

$$g[\omega(q,j)]=\frac{1}{N\hbar\omega(q,j)}\left\{\frac{1}{\exp[\hbar\omega(q,j)/kT]-1}+1\right\}, \quad (3)$$

where N is the number of unit cells, R is the recoil energy of a free emitting atom, $\hbar$ is Planck's constant divided by 2π, k is the Boltzmann constant, T is the absolute temperature, $\mathbf{q}$ is the propagation vector, and j is the polarization of a vibrational wave of the crystal. α refers to the specific lattice from which the γ ray is being emitted or absorbed, ϱ^α is a unit vector in the direction of emission of the γ ray, $\mathbf{e}^\alpha(q,j)$ is the polarization vector of the vibrational wave.

The purpose of this paper is to provide accurate theoretical values for the Debye-Waller factor for white tin in the temperature region of the harmonic approximation. Calculations of this type are necessary in order to determine the extent to which the existing theory agrees with experimental results.[4] In this paper, Eq.(2) is evaluated using the theoretical frequency spectrum and polarization vectors for white tin calculated from the elastic data.

In a previous paper,[5] referred to as WLD, the frequency spectrum for white tin was calculated using the elastic constants reported by Mason and Bömmel.[6]

In this paper we also calculate the frequency spectrum using the elastic constants of Rayne and Chandrasekhar.[7] In Sec. II the dynamic matrix for the acoustic frequencies is obtained including the interaction of the optical motion. In the long-wavelength limit this matrix reduces to an effective elastic matrix in which the effect of the relative motion of the two sublattices is retained. The method of calculation with the resulting dispersion curves is also presented.

In Sec. III, the constant $2W$ is expressed as a quadratic function of the components of ϱ^α. The method and results of our calculations are presented in Sec. IV.

II. EFFECT OF OPTICAL MOTION ON THE ACOUSTIC MATRIX

In this section we consider the interaction of the optical and acoustical modes and show that the acoustic frequencies are in general depressed. This depression can be understood in terms of a mixing of relative sublattice motion into the "pure" acoustic motion in which the two sublattices are moving as a unit. In the long-wavelength (L-W) limit the optic-acoustic interaction is proportional to q^4 for crystals with an inversion center but proportional to q^2 otherwise. Consequently, the elastic properties of crystals without an inversion center, such as white tin, will contain an optic-acoustic interaction term while crystals with an inversion center will not. In this section we obtain the corrected L-W acoustic matrix.

In WLD, the form of the dynamic matrix for white

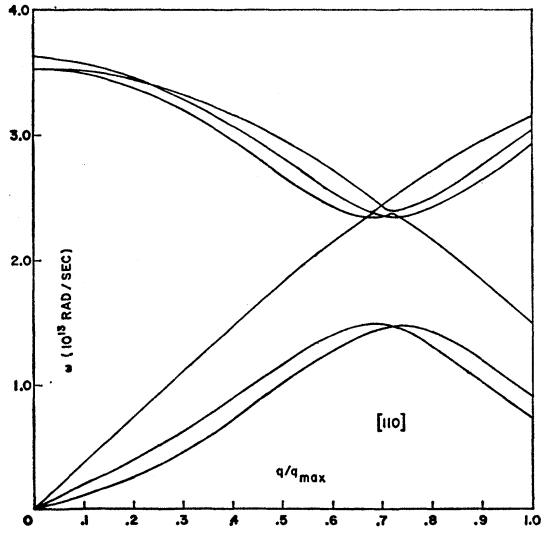

FIG. 2. Dispersion curves for white tin along [110] direction in the Brillouin zone using Rayne and Chandrasekhar elastic data.

[4] A rough order of magnitude calculation of the anisotropy ratio for tin in agreement with our results has been reported recently by Yu. Kagan. [Dokl. Akad. Nauk SSSR **140**, 794 (1961) [translation: Soviet Phys.—Doklady **6**, 881 (1962)]]. However, in view of the methods used by Kagan in evaluating this ratio, we conclude that this agreement is accidental, inasmuch as the optical modes were not included. Kagan's expressions require a detailed knowledge of the density of states—a quantity not to be obtained in any simple manner analytically for a real crystal. His density of states is derived from a simplified nearest neighbor lattice dynamics model in which the dynamical matrix is diagonal and consequently inconsistent with the elastic-dynamic matrix. In addition, the model does not apply to the actual structure of tin. Having omitted the optical mode contributions, the expressions derived are not valid since the optical modes contribute significantly, particularly at low temperatures as is shown from specific heat data and by our detailed calculations.

[5] T. Wolfram, G. W. Lehman, and R. E. DeWames, Phys. Rev. **129**, 2483 (1963).

[6] W. P. Mason and H. E. Bommel, J. Acoust. Soc. Am. **28**, 930 (1956).

[7] J. A. Rayne and B. S. Chandrasekhar, Phys. Rev. **120**, 1658 (1960).

tin in the center-of-mass system was discussed. The dynamic equations in this system are

$$\mathfrak{D}(q)\begin{pmatrix}\mathbf{x}_1\\ \mathbf{x}_2\end{pmatrix}=\omega^2\begin{pmatrix}\mathbf{x}_1\\ \mathbf{x}_2\end{pmatrix}, \tag{4}$$

where $\mathfrak{D}(q)$ is the dynamic supermatrix in the center-of-mass system with elements

$$\begin{aligned}\mathfrak{D}_{11}(\mathbf{q})&=D_{11}+\mathrm{Re}D_{12},\\ \mathfrak{D}_{12}(\mathbf{q})&=\mathfrak{D}_{21}(q)=-\mathrm{Im}D_{12},\\ \mathfrak{D}_{22}(\mathbf{q})&=D_{11}-\mathrm{Re}D_{12},\end{aligned} \tag{5}$$

and the D_{ij} are 3×3 supermatrices described in WLD. The vector $\mathbf{x}_1$ is the "pure" acoustical (in-phase) motion of the two sublattices and $\mathbf{x}_2$ is the "pure" optical (out-of-phase) motion. Using partitioning, we obtain the dynamic equations for the acoustic frequencies

$$\{(\mathfrak{D}_{11}-\omega^2)-\mathfrak{D}_{12}(\mathfrak{D}_{22}-\omega^2)^{-1}\mathfrak{D}_{12}\}x_1=0. \tag{6}$$

This equation is exact and shows that the acoustic frequencies are lowered by the presence of optical modes. The eigenvalues of $\mathfrak{D}_{11}$ and $\mathfrak{D}_{22}$ are the "pure" acoustical and optical frequencies, respectively. $\mathfrak{D}_{12}$ is the optic-acoustic interaction matrix. As $\mathbf{q}\rightarrow0$ the eigenvalues of $\mathfrak{D}_{11}$ and $\mathfrak{D}_{12}$ vanish. The matrix $\mathfrak{D}_{22}$, however, approaches a diagonal form with large constant eigenvalues, the optical frequencies. $(\mathfrak{D}_{22}-\omega^2)^{-1}$ can be expanded in a power series in $\mathfrak{D}_{22}^{-1}$,

$$(\mathfrak{D}_{22}-\omega^2)^{-1}=\mathfrak{D}_{22}^{-1}+\omega^2\mathfrak{D}_{22}^{-2}+\omega^4\mathfrak{D}_{22}^{-3}+\cdots. \tag{7}$$

This series converges very rapidly in the L-W limit since $[\omega\rightarrow0]$ while the eigenvalues of $\mathfrak{D}_{22}$ approach 10^{26} sec^{-2}. In the elastic limit one retains only terms of order q^2 so that the acoustic matrix reduces to

$$\{(\mathfrak{D}_{11}-\omega^2)-\mathfrak{D}_{12}\mathfrak{D}_{22}^{-1}\mathfrak{D}_{12}\}_{q\rightarrow0}. \tag{8}$$

The interaction matrix, $\mathfrak{D}_{12}$, is proportional to q^2 for crystals with an inversion center and consequently the second term in Eq. (8) is proportional to q^4 and may be neglected. On the other hand, for crystals without a center inversion, $\mathfrak{D}_{12}$ is proportional to $\mathbf{q}$ so that the optic-acoustic correction must be retained. Physically, however, we expect the correction to be small compared to "pure" acoustic frequencies. In WLD, the frequency spectrum for white tin was calculated using the elastic constants reported by Mason and Bömmel (see Table I). In this case the correction term could be ignored since it caused only negligible corrections (about 3%). The elastic constants reported by Rayne and Chandrasekhar,[7] (see Table I) also by House and Vernon,[8] imply in our model a much larger optic-acoustic interaction. In addition, these constants give rise to a much lower transverse acoustic branch along the [110] direction. Consequently, it is necessary to use Eq. (8) to determine the atomic force constants. Equating Eq. (8) to the elastic matrix as discussed in WLD yields quadratic algebraic equations relating the atomic force constants to the elastic constants. The value of ω_{av} and t were chosen according to the procedure in WLD. The A-S atomic force constants for the two calculations are given in Table II.

Using the elastic data of Mason and Bömmel it was possible to satisfy all equations within the experimental error in the elastic constants. However, with the elastic data of Rayne and Chandrasekhar, it was not possible to obtain total consistency among all the equations. This resulted because the A-S model implies that

$$C_{44}-C_{13}-C_{66}+C_{12}=0. \tag{9}$$

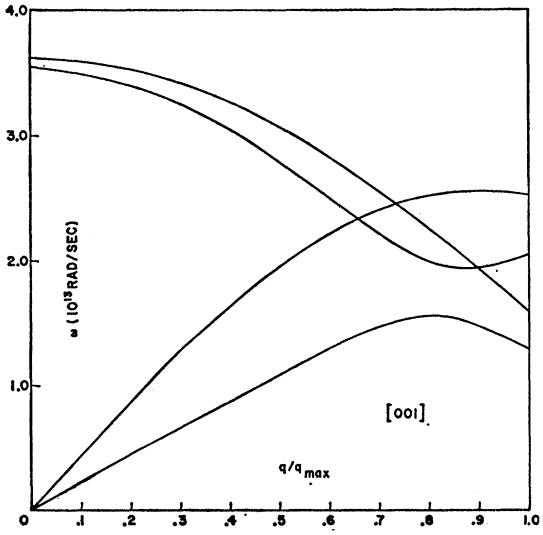

FIG. 3. Dispersion curves for white tin along [001] direction in the Brillouin zone using Rayne and Chandrasekhar elastic data.

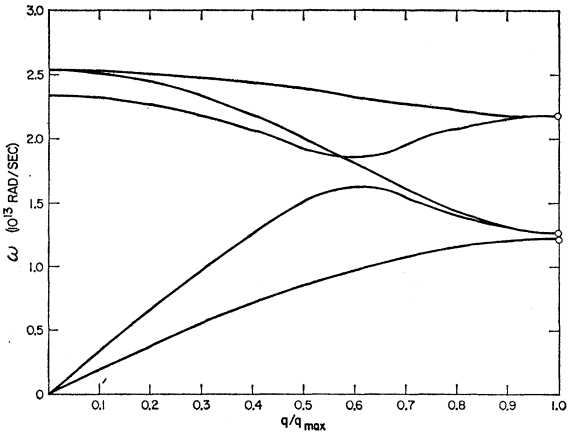

FIG. 4. Dispersion curves for white tin along [100] direction in the Brillouin zone using Mason and Bömmel elastic data.

[8] D. G. House and E. V. Vernon, Brit. J. Appl. Phys. **11**, 254 (1960).

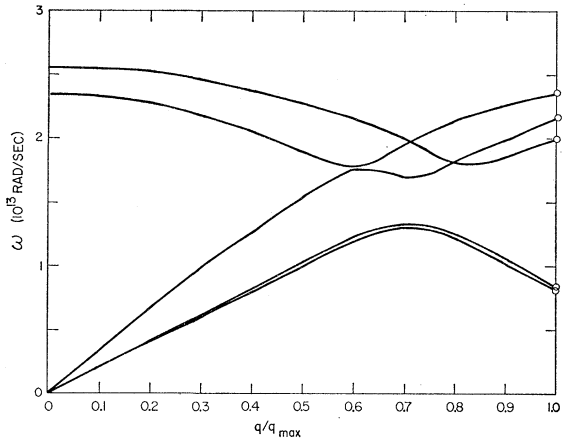

FIG. 5. Dispersion curves for white tin along [110] direction in the Brillouin zone using Mason and Bömmel elastic data.

This condition is well satisfied for the constants of Mason and Bömmel, but for Rayne and Chandrasehkar's data it is not.

The effect of the inconsistency is to lower the quasi-transverse branch by 40% and raise the quasilongitudinal branch by 10% along the [101] direction. All other branches along the principal directions including the pure transverse branch along the [101] direction are unaffected.

The resulting dispersion curves are shown in Figs. 1–3. For comparison Figs. 4–6 show the dispersion curves obtained in WLD. The value of the optical frequencies at $\mathbf{q}=\mathbf{0}$ are larger than in WLD. This is necessary in order to keep the optic-acoustic interaction small. In order to remove the condition on the elastic constants imposed by the A-S model one needs to consider a full tensor force model. This, however, will introduce more parameters which obviously could not be determined without experimental dispersion curves. In WLD it is shown that, for any atomic force model, it is necessary to include at least fourth neighbors in order to be consistent with elastic theory.

III. $2W$ FOR WHITE TIN

White tin has a body-centered tetragonal structure with two atoms per unit cell. The structure is two interpenetrating body centered tetragonal lattices with lattice basis $(0,0,0)$, $(0,\frac{1}{2},\frac{1}{4})$. The superscript α is left out in what follows since the constant $2W$ must be the same for either lattice.

Equation (2) can be expressed as an inner product

$$2W=R(\rho,H\rho), \qquad \rho=(\rho_x,\rho_y,\rho_z), \tag{10}$$

where the elements of the H matrix are given by

$$H_{n,m}=\sum_q \sum_j g[\omega(q,j)]\mathbf{e}_n(q,j)\mathbf{e}_m{}^*(q,j). \tag{11}$$

TABLE I. Room temperature elastic constants for white tin (in units 10^{11} dyn cm^{-2}).

Constants	Mason and Bömmel	Rayne and Chandrasekhar
C_{11}	7.33	7.23
C_{33}	8.74	8.840
C_{44}	2.19	2.203
C_{66}	2.25	2.400
C_{12}	2.38	5.94
C_{13}	2.48	3.58

When the coordinate axes are chosen to lie along the principal axis of the crystal, $2W$ must be a quadratic function of the components of ϱ. Hence,

$$2W=R\{\rho_x{}^2H_{xx}+\rho_y{}^2H_{yy}+\rho_z{}^2H_{zz}\}, \tag{12}$$

or

$$=R\{(\rho_x{}^2+\rho_y{}^2)H_{xx}+\rho_z{}^2H_{zz}\}, \tag{13}$$

since the crystal has a fourfold axis of symmetry. It is convenient to express Eq. (13) in the form

$$2W=RH_{zz}(T)\{\epsilon(T)-\mu^2[\epsilon(T)-1]\},$$

where $\epsilon(T)=H_{xx}(T)/H_{zz}(T)$, $\mu=\cos\theta$, θ is the angle between ϱ and the principal axis.

IV. RESULTS

In order to calculate the constant $2W$ the vibration frequencies and polarization vectors for an arbitrary propagation vector $\mathbf{q}$ were determined using the axially symmetric lattice dynamics model described in a previous paper.[9]

The H_{xx} and H_{zz} matrix elements [Eq. (11)] were evaluated by integrating over $\frac{1}{16}$ of the Brillouin zone appropriate to white tin. This portion of the Brillouin zone was divided into two regions which were transformed into unit cubes by nonlinear transformations. A triple Gaussian quadrature was used to evaluate the resulting integrals.

The 6×6 dynamical matrix for white tin was diagonalized by a 2×2 Jacobi rotation procedure at 1024 points in each region. The polarization vectors for

TABLE II. A–S force constants (in units of 10^4 dyn cm^{-1}).

Constants	I[a]	II[b]
K_1 (1,12)	0.9183	0.2945
C_2 (1,12)	1.515	1.472
K_1 (2,11)	1.757	1.551
C_2 (2,11)	0.7575	−0.7362
K_1 (3,12)	1.276	2.446
C_2 (3,12)	−0.736	0.7404
K_1 (4,11)	0.4206	0.7054
C_2 (4,11)	−0.1979	−0.6688

[a] Using Mason and Bömmel elastic data.
[b] Using Rayne and Chandrasekhar elastic data.

[9] G. W. Lehman, T. Wolfram, and R. E. DeWames, Phys. Rev. 128, 1593 (1962).

TABLE III. Comparison of experimental and calculated values for the polycrystal Debye-Waller factor.

T(°K)	Wiedemann[a] *et al.*	Boyle *et al.*	Barloutand[b] *et al.*	Alekseyevsky *et al.*	I[c]	II[d]	Debye model $\theta_D=142$°K
4	(0.53), (0.60)				0.63	0.61	0.73
20	(0.52), (0.59)				0.61		0.70
77	(0.39), (0.40)	(0.40)		(0.32 ±0.06)	0.40	0.37	0.46
90			(0.30±0.07), (0.32±0.015)				
150		0.22			0.22	0.18	
300		0.035		(0.061±0.015)	0.053	0.036	0.07
400		0.009				0.011	
500		0.002			0.008	0.004	0.012

[a] W. H. Wiedemann, P. Kienle, and F. Pobell, Z. Physik **166**, 109 (1962).
[b] R. Barloutand, J. O. Picon, and C. Tzara, Compt. Rend. **250**, 2705 (1960).
[c] Using Mason and Bömmel elastic data.
[d] Using Rayne and Chandrasekhar elastic data.

points lying outside the fundamental $\frac{1}{16}$ of the Brillouin zone were obtained by means of symmetry operations of the D_{4h} group. Several checks were made to insure that our values of $H_{m,m}$ were independent of order of the Gaussian quadrature.

The experimental and calculated temperature dependence of the polycrystalline Debye-Waller factor is given in table III showing good agreement from 0 to 300°K. The values calculated using Rayne and Chandrasekhar's elastic data seem to give the best over-all fit; however, with the present experimental accuracy it does not seem possible to select between the two calculations. For comparison, the temperature dependence of Debye-Waller factor calculated from the Debye approximation with $\theta_D=142$°K, as suggested in a previous analysis[10] is also shown in Table III. Clearly, our results indicate that the Debye model does not give a good representation of the frequency spectrum of tin and that one is not justified in accounting for the difference between experimental values and calculated values using the Debye approximation by introducing higher order corrections such as anharmonicities. The deviation of experimental values from calculated values using A-S model above 300°K can now probably be attributed to higher order corrections. The effect of anharmonicities is presently being investigated.

TABLE IV. Temperature dependence of $H_{zz}(T)$ and $\epsilon(T)$.

T(°K)	$H_{zz}(T)$[a] (in units of 10^3 eV^{-1})	$\epsilon(T)$[a]	$H_{zz}(T)$[b] (in units of 10^3 eV^{-1})	$\epsilon(T)$[b]
4	0.169	1.106	0.174	1.106
6	0.170	1.106	0.175	1.106
15	0.175	1.109	0.183	1.109
50	0.233	1.15	0.260	1.14
77	0.304	1.17	0.345	1.15
150	0.526	1.19	0.606	1.16
300	1.01	1.2	1.17	1.17
400	1.34	1.2	1.56	1.17
500	1.68	1.2	1.95	1.17

[a] Using Mason and Bömmel elastic data.
[b] Using Rayne and Chandrasekhar elastic data.

[10] A. J. F. Boyle, D. St. P. Bunbury, C. Edwards, and H. E. Hall, Proc. Phys. Soc. (London) **A77**, 129 (1961).

The temperature dependence of the function $H_{zz}(T)$ and the anisotropy ratio $\epsilon(T)$ is given in Table IV. The anisotropy ratio is found to be only slightly temperature sensitive in agreement with Kagan's results.[4]

We are currently aware of two recent attempts at measuring the anisotropy ratio of $f_x/f_z=e^{-RH_{xx}}/e^{-RH_{zz}}$. One of these measurements has been attempted by Alekseyevsky *et al.*[11] and their conclusion is that $f_x/f_z=1.4$ over the whole temperature range. Their calculated f_x/f_z was determined from experimental data corrected for quadrupole effects.

It is apparent that the conclusions of Alekseyevsky *et al.* are in disagreement with our theoretical prediction. In fact, their conclusions that $f_x/f_z=1.4$ over the 80–300°K range imply that the ansiotropy ratio $\epsilon(T)$, is not only strongly temperature dependent but increases as the temperature increases, which implies that the lattice anisotropy is decreasing as the temperature increases. This is difficult to believe because if the mean square displacement along the [001] is larger at low

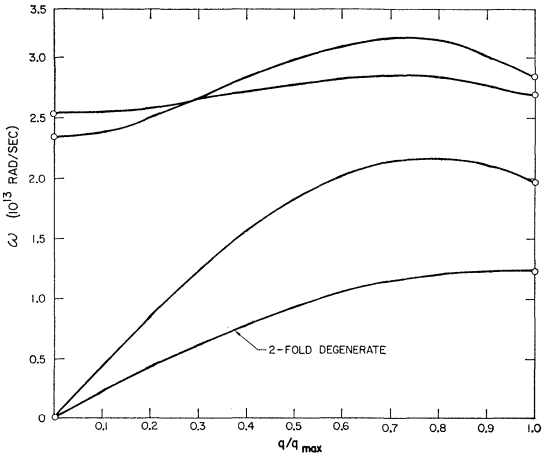

FIG. 6. Dispersion curves for white tin along [001] direction in the Brillouin zone using Mason and Bömmel elastic data.

[11] N. E. Alekseyevsky, Pham Zuy Hien, V. G. Shapiro, V. S. Shunel, Zh. Eksperim. i Teor. Fiz. **43**, 790 (1962) [translation: Soviet Phys.—JETP **16**, 559 (1963)].

temperatures than that along the [100] direction in the harmonic region one would expect their ratio to be an increasing function of temperature (since the functional dependence on frequency goes from $\langle 1/\omega \rangle$ to $\langle 1/\omega^2 \rangle$ at high temperatures). Furthermore, the thermal expansion data show that the thermal expansion coefficient along the [001] is higher than along the [100]; this should still further increase the difference.

The other measurement is that of Meechan *et al.*[12] of our laboratory who have obtained essentially the same value for f_x/f_z at room temperature but no measurable difference for f_x/f_z at 100°K.

This experimental discrepancy must be resolved before we can make meaningful comparison between theory and experiment.

TABLE V. Comparison of experimental and calculated values of the Debye-Waller factor along three crystal axes.

			A–S model			
	Alekseyevsky *et al.*		I[a]		II[b]	
T(°K)	77	293	77	293	77	293
[001]	0.24±0.05	0.054±0.01	0.46	0.074	0.41	0.05
[101]		0.072±0.01		0.05		0.033
[100]	0.36±0.06	0.076±0.01	0.39	0.045	0.36	0.03

[a] Using Mason and Bömmel elastic data.
[b] Using Rayne and Chandrasekhar elastic data.

The experimental and calculated angular dependence of the Mössbauer intensity for several temperatures is shown in Table V. The anisotropy ratios are compared in Table VI. Table VII gives the calculated and experimental specific[13] heat from 1 to 300°K. As expected, the calculated specific heat values using Rayne and Chandrasekhar's elastic data is slightly higher than that calculated using Mason and Bömmel's elastic data.

[12] C. J. Meechan, A. H. Muir, U. Gonser, H. Wiedersich, Bull. Am. Phys. Soc. 7, 600 (1962).
[13] C. A. Shiffman, The Heat Capacities of the Elements below Room Temperature, General Electric Research Laboratory (unpublished).

TABLE VI. Comparison of experimental and calculated values of the anisotropy ratio $\epsilon(T)$.

	$\epsilon(T)$		
	Alekseyevsky	A–S model	
T(°K)	*et al.*	I[a]	II[b]
77	0.715	1.17	1.15
300	0.883	1.2	1.17

[a] Using Mason and Bömmel elastic data.
[b] Using Rayne and Chandrasekhar elastic data.

Between 6–15°K the calculated values are low. It was impossible to raise the lattice contribution to the specific heat in that temperature range without changing the low temperature agreement of C_v and the Debye-Waller factor.

TABLE VII. Comparison of experimental and calculated values for the total specific heat of white tin[a] (in units of cal mole^{-1} deg^{-1}).

T(°K)	C_v(exp)	C_v(I)[b]	C_v(II)[c]
1	0.00046	0.00042	0.00045
2	0.0014	0.0011	0.0015
3	0.0032	0.0027	0.0042
4	0.0067	0.0053	0.0074
6	0.036	0.015	0.021
15	0.64	0.25	0.29
50	3.68	3.10	3.08
150	5.85	5.55	5.53
300	6.3	5.97	5.97

[a] $\gamma = 3.5 \times 10^{-4}$ cal mole^{-1} deg^{-1}.
[b] Using Mason and Bömmel elastic data.
[c] Using Rayne and Chandrasekhar elastic data.

ACKNOWLEDGMENTS

The authors are particularly indebted to C. J. Meechan and A. H. Muir for numerous discussions concerning the experimental work on Sn. We also wish to acknowledge discussions with M. H. Cohen, U. Gonser, V. Heine, and H. Wiedersich on the subject matter of this paper.